

Material Characterization of Pultruded Laminates and Shapes

S. S. SONTI AND E. J. BARBERO*

Constructed Facilities Center

West Virginia University

Morgantown, WV 26506-6103

ABSTRACT: This paper discusses the material characterization of wide flange pultruded structural shapes (E-glass, Vinylester). The material was subjected to three loading conditions: tension, shear, and bending. Coupon samples were obtained from web and flanges of the I-section for tension and shear tests. Tensile properties were obtained from rectangular coupons with end tabs loaded in tension to failure. Shear properties were obtained from two different test methods: Iosipescu shear test method and torsion of rectangular samples. Experimentally determined material properties were compared to analytical predictions based on micro and macromechanics. Micromechanical models are used for the prediction of individual laminae (roving layers, continuous strand mat, nexus veils) properties. Classical lamination theory (CLT) is then used to predict the laminate properties. In addition, I-beams were tested in bending to evaluate their response and the experimental results were compared to predictions using Mechanics of Laminated Beams (MLB) approach. Results indicate a good correlation between experimental data and theoretical predictions, showing that the properties of pultruded composites can be predicted with sufficient accuracy. The superiority of the torsion test for determination of in-plane shear stiffness is demonstrated.

INTRODUCTION

A GROWING TREND towards using composite materials for Civil Infrastructure systems applications highlights the need for efficient means of predicting and evaluating their material properties. Civil engineering applications are dominated by traditional materials like steel and concrete, but use of composites are being considered (GangaRao et al., 1991; Barbero et al., 1991; Ahmad et al., 1989; Iyer, 1991). Unlike aerospace related applications, composites to be used in high-volume structural applications (bridges, highways, etc.) need to be cost-effective, yet structurally efficient. A cost-effective operation would comprise of a low cost manufacturing process and a combination of low cost fibers and resins. Pultrusion in a low-cost operation with high production rates and is being used for the production of structural components. Low cost E-glass fibers and vinylester or

*Author to whom correspondence should be addressed.

polyester resins are being used as the material constituents. Current standard structural shapes (I-beams, box-beams, cellular sections, etc.) use E-glass and vinylester or polyester resins.

The aim of this study is to perform stress analysis on pultruded composite beams taking into account that low cost structural RP materials are usually produced by pultrusion. Because of manufacturing constraints, pultruded profiles of existing shapes with specified materials systems, available from Creative Pultrusions, Inc. (Creative Pultrusions, 1988) are used in this study. A wide flange I-beam was chosen for the analysis as this is one of the most commonly used structural component. The primary constituents in this product are E-glass fibers and Vinylester resin. Glass reinforcements are widely used for structural applications due to its low cost. Among the available compositions: E-glass, S-glass, C-glass, A-glass, M-glass, D-glass and L-glass; E-glass is widely used in structural applications. It is a low-alkali composition (aluminum borosilicate) exhibiting excellent electric insulation properties. Vinylester resins are thermosetting resins consisting of a polymer backbone with acrylate ($R=H$) or methacrylate ($R=CH_3$) termination. Due to their chemical resistance, they are fabricated into fiberglass reinforced plastic (RP) composites via filament winding, hand lay-up, bag molding or pultrusion.

OBJECTIVE OF THIS STUDY

The major objectives of this study are: (1) experimental determination of laminate properties (coupon level) and their validation using an integrated micro-mechanics and macromechanics approach; and (2) experimental determination of the bending behavior (component level) of I-sections under 3-point bending and its validation using MLB.

A $8'' \times 8'' \times 0.375''$ wide-flange I-beam was chosen for coupon and component testing. The laminate properties obtained from coupon tests are: longitudinal stiffness and strength (E_x, X_t), transverse stiffness and strength (E_y, Y_t), Poisson's ratio (ν_{xy}, ν_{yx}) and in-plane shear stiffness and strength (G_{xy}, S). The I-section was tested in bending to obtain the beam stiffness E .

The experimental properties obtained were compared to the analytical predictions. The laminate properties were predicted using an integrated micro/macro mechanics approach where the lamina properties are obtained using micro-mechanics followed by classical lamination theory (CLT) for the laminate. The beam behavior was predicted using Mechanics of Laminated Beams (MLB).

TENSION TESTS

Tension tests were performed on laminate samples obtained from flanges and web of the I-section to determine the longitudinal and transverse stiffness and strength properties.

Longitudinal properties (E_x, X_t): Thirty-four rectangular coupons were obtained in two sizes from the flanges and web of the I-section: $18'' \times 2'' \times 0.375''$ (8 flange, 8 web) and $8'' \times 1'' \times 0.375''$ (8 flange, 10 web). The coupons were cut in the direction of the axis of the beam. Aluminum tabs were bonded at the

Materi

grippin
(Magn
thickn
gage r
conditi
gradua
were r
Hooke

where
and A
tudinal
from,

where
For
were l
of the s
can be

where

$X_t =$
 $P_{ult} =$
 $A_c =$

In the
tensile
sion.

Tran
I-sectio
(7'' ×
using a
one in
gitudin
modul

gripping ends to avoid damage of the composite at the grips. Epoxy adhesive (Magnabond 56) and a tight clamping device were used to reduce the bondline thickness. A Baldwin machine was used for the tension test. A 3-element strain gage rosette was bonded to the specimen and the output hooked to a strain gage conditioner and amplifier system in a quarter bridge circuit. The specimen is gradually loaded and the strains in the longitudinal, transverse and 45° direction were recorded. The tensile modulus in the fiber direction was obtained using Hooke's law,

$$\sigma_x = E_x \epsilon_x \quad (1)$$

where σ_x is the applied stress which is obtained as $\sigma_x = P/A$, where P is the load and A the cross-sectional area of the specimen. The strain recorded in the longitudinal direction is used in Equation (1). The major Poisson ratio ν_{xy} is obtained from,

$$\nu_{xy} = \frac{\epsilon_x}{\epsilon_y} \quad (2)$$

where ϵ_x is the strain in fiber direction and ϵ_y is the strain in transverse direction.

For the determination of strength in the fiber direction the coupon samples were loaded until failure. The ultimate load divided by the area of cross section of the specimen gives us the tensile strength. Tensile strength in the fiber direction can be predicted by,

$$X_t = \frac{P_{ult}}{A_c} \quad (3)$$

where

X_t = longitudinal tensile strength

P_{ult} = ultimate load at failure

A_c = area of the cross section of the laminate

In the above formula, the area of the roving layers only is considered because the tensile strength is mainly controlled by the fibers due to their high strength in tension.

Transverse properties (E_y, Y_t): A total of 15 coupons were obtained from the I-section. Eight from the flange (3.5" × 1") and seven from the web (7" × 1"). The coupons were tested in a Instron machine and the data recorded using a strain gage conditioner and amplifier system. Two strain gages were used: one in the longitudinal (transverse material) direction and one in transverse (longitudinal material) direction. In the longitudinal (transverse material) direction modulus is determined using,

$$\sigma_y = E_y \epsilon_y \quad (4)$$

Table 1. Stiffness comparison for flange samples.

Material Property	Experimental		Analytical Prediction
	Mean Value	Number of Samples	
$E_x \times 10^6$ (psi)	2.936	16	2.585
$E_y \times 10^6$ (psi)	1.650	8	1.646
$G_{xy}^a \times 10^6$ (psi)	0.484	10	0.598
$G_{xy}^b \times 10^6$ (psi)	0.552	5	0.598
ν_{xy}	0.275	16	0.392
ν_{yx}	0.193	8	0.249

^aResults from Iosipescu shear tests.

^bResults from torsion tests.

The minor Poisson's ratio is obtained from,

$$\nu_{yx} = -\frac{\epsilon_y}{\epsilon_x} \quad (5)$$

The smaller size of the flange samples in the transverse direction was chosen to avoid the flange-web intersection, thus allowing only 4" on each half of the flange. In the web, longer samples could be obtained due to the shape of the I-beam which allows about 7" in the transverse direction of the web.

Composites, very strong in the fiber direction, are usually very weak in the transverse direction. The strength in the transverse direction is determined from coupons (3.5" × 1") obtained from the web and flanges by testing them to failure using the relation,

Table 2. Stiffness comparison for web samples.

Material Property	Experimental		Analytical Prediction
	Mean Value	Number of Samples	
$E_x \times 10^6$ (psi)	2.620	18	2.474
$E_y \times 10^6$ (psi)	1.580	7	1.597
$G_{xy}^a \times 10^6$ (psi)	0.651	8	0.581
$G_{xy}^b \times 10^6$ (psi)	0.566	5	0.581
ν_{xy}	0.288	18	0.392
ν_{yx}	0.176	7	0.253

^aResults from Iosipescu shear tests.

^bResults from torsion tests.

where

$$Y_t = \text{tr}$$

$$P_{ult} = \text{ul}$$

$$A_c = \text{ar}$$

Test res
compar
 E_x, E_y, C
the result

In-plan
methods.
the torsio
Iosipes
flange, 8
the shear
test fixtur
signed W

Table 3. Strength comparison for flange samples.

Material Property	Experimental		Analytical Prediction (psi)
	Mean Value (psi)	Number of Samples	
X_t	36,037.45	16	37,600.00
Y_t	10,922.35	8	11,546.66
S	10,819.05	10	8,533.00

$$Y_t = \frac{P_{ult}}{A_c} \quad (6)$$

where

Y_t = transverse tensile strength

P_{ult} = ultimate load at failure

A_c = area of the composite or the area of cross-section

(5)

Test results: Results of the tension tests were provided in Tables 1–4 which are compared with the analytical predictions. Tables 1 and 2 provide the results of E_x , E_y , G_{xy} , ν_{xy} , and ν_{yx} for the flange and web samples. Tables 3 and 4 provide the results of X_t , and Y_t for the flange and web samples respectively.

SHEAR TESTS

In-plane stiffness and strength were determined using Iosipescu and torsion test methods. The Iosipescu test was used for the stiffness and strength properties but the torsion test was used only for stiffness evaluation.

Iosipescu shear test (G_{xy} , S): Eighteen samples, 3" \times 0.75" \times 0.75" (10 flange, 8 web), were obtained from the web and flanges of the I-beam to evaluate the shear properties using the Iosipescu shear test method (Iosipescu, 1967). A test fixture was fabricated at West Virginia University on the lines of the redesigned Wyoming fixture (Adams and Walrath, 1987). The shear test fixture was

Table 4. Strength comparison for web samples.

Material Property	Experimental		Analytical Prediction (psi)
	Mean Value (psi)	Number of Samples	
X_t	34,151.55	18	33,600.00
Y_t	11,867.42	7	11,653.00
S	10,195.47	8	8,720.00

used in a testing machine set up in a compression mode to test specimens 0.75 in. wide allowing a variation of 0.04 inch on that width. The fixture comprises of two identical halves of which the left half is fixed to the base, and the right half moves up and down on four posts and a recirculating ball bushing. The right half of the fixture is so designed to be easily attached to the crosshead of a testing machine. The crosshead holds and positions the fixture and the specimen can be easily installed. The advantage of using this fixture is that the front face of the specimen remains visible during the test and failure progression can be monitored visually. This test induces a state of uniform shear stress at the midsection of the specimen by creating two counteracting moments which are produced by the applied loads. As suggested by many researchers, the loading points were located away from the notch edge. Adams et al. (1987) indicated that loading points too close to the notches caused the influence of concentrated loadings to spread into the gage section region. Also, Spigel et al. (1987) found that for the determination of shear modulus, where the strains are measured near the center of the specimen, moving the load away from the notch edge resulted in a more uniform state of shear and therefore a more accurate shear modulus value.

For the tests conducted, shear strains were measured by using a ± 45 degree two-element strain gage bonded at the center of the coupon between the notches (Figure 1). After balancing and calibrating the compression load cell of the Instron machine, the coupon is placed into the fixture and fastened with the trapezoidal blocks by tightening the screws. After the coupon is set and the entire fixture is aligned with the loading axis, the fixture is fastened on the load cell and the bonded strain gages are balanced with the strain conditioner. The test was performed at a loading rate of 0.02 in./min. The differential voltage output, transferred into the strain conditioner and through quarter bridge configuration

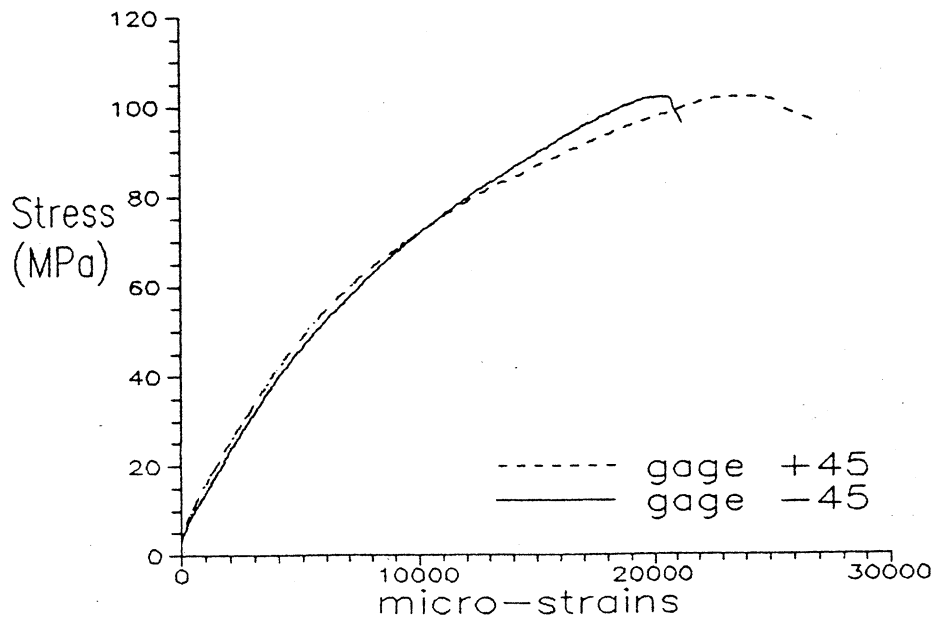


Figure 1. Stress-strain curve for an losipescu specimen.

and signal
produces p

where

τ_{xy} = shea

P = app

A_{n0} = area

For a pla
for shear st

From Equa

The shear

Torsion
from the fl
loading rat
assess the
ticlockwis
reacting an
hooked to
measured
hooked to
in Figure 2
tion for or
material (I

where

d = width

t = depth

L = gage

and signal amplification, is recorded by a data acquisition system. As the load produces pure shear applied shear stress is given by,

$$\tau_{xy} = P/A_{n0} \quad (7)$$

where

- τ_{xy} = shear stress
- P = applied load
- A_{n0} = area of the cross section between the notches.

For a plane strain problem, with an orientation of 45 degrees, the expression for shear strain is obtained as,

$$\gamma_{xy} = \epsilon_{45} - \epsilon_{-45} \quad (8)$$

From Equations (7) and (8) the shear modulus G_{xy} can be given as,

$$G_{xy} = \frac{\tau_{xy}}{\gamma_{xy}} \quad (9)$$

The shear strength can be obtained as,

$$S = P/A_{n0} \quad (10)$$

Torsion test (G_{xy}): Ten (7" × 1") samples were used that were obtained from the flanges and web of the I-beam. Torque was applied on the samples at a loading rate of less than 3 degrees per minute both in loading and unloading. To assess the effect of possible misalignment we applied both clockwise and anticlockwise twisting. The moment was computed from the displacement of the reacting arm on a torsion machine, displacement that was measured by a LVDT hooked to a computerized data acquisition system. The twisting angle was measured on a gage length of 11.17 in. as the difference between two LVDT's hooked to the data acquisition system. A typical torque vs. angle of twist is shown in Figure 2. The shear modulus was computed using the Lekhnitskii torsion solution for orthotropic rectangular plates, specialized for a transversely isotropic material (Davalos, 1991). The formula used is,

$$K = \frac{T}{\theta} = \frac{G_{12} dt^3}{L} k \quad (11)$$

where

- d = width of the sample
- t = depth of the sample
- L = gage length

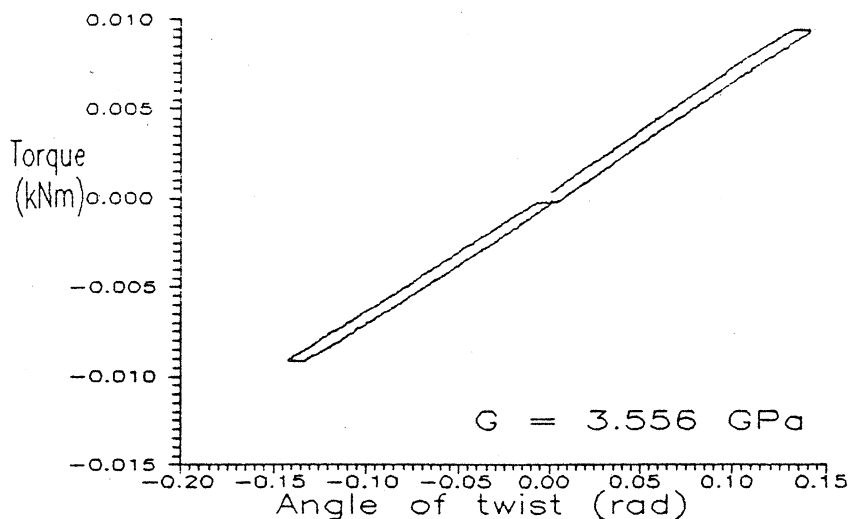


Figure 2. Typical torque vs. angle of twist curve for a torsion test.

T = Torque

θ = angle of twist

k = constant depending on the width-to-depth ratio of the cross section
(Timoshenko and Goodier 1988)

Test results: Iosipescu and Torsion shear test results are shown in Tables 1–4. The in-plane shear modulus and strength are computed as explained in the above section. The value of the shear stiffness varied from 0.3×10^6 psi to 0.7×10^6 psi for the Iosipescu samples, but for the torsion samples it varied between 0.51×10^6 psi to 0.59×10^6 psi. There is scatter in the results of the Iosipescu tests which can be attributed to the variability in the material in the notch region. During the Iosipescu test we are concentrating on a very small area for the material property and the stiffness will vary depending on whether it is a fiber rich or a resin rich area. Results for the shear stiffnesses from the torsion tests showed greater consistency than the Iosipescu results. In the torsion tests, the property measured is the average over a certain length of the specimen. Better consistency of the results makes it an economic alternative over Iosipescu tests for the determination of shear stiffness. For the shear strength, only the Iosipescu tests were used.

BENDING TESTS

Three-point bending tests were conducted on the I-beams in seven different span lengths: 4, 6, 10, 12, 14, 16, and 18 ft respectively. The specimen is supported on two concrete blocks simulating a simple-support boundary condition. Lateral supports were used to prevent any lateral-torsional buckling. The load is applied at the mid-span by an overhung hydraulic jack. The load is measured using a portable strain indicator and the central deflection using a ± 2 in. LVDT, both sensors connected a computerized data acquisition system (DAS). The

Material

deflectio
LVDTs.

where

P = loa

L = spa

I = mo

w = exp

Test re

different
thus obta

Based o
and mac
(coupons
tensile m
of the vi
rods and
and shear

Knowin
volume fr
ical prop
removal b
Various o

deflections were also measured using dial gages to check the accuracy of the LVDTs. The beam stiffness was computed using:

$$E_{test} = \frac{PL^3}{48Iw} \quad (12)$$

where

- P = load
- L = span length
- I = moment of inertia
- w = experimental deflection

Test results: The experimental stiffness of the beams obtained for the seven different spans are shown in Table 5. The experimental beam stiffnesses (E_{test}) thus obtained are compared to the predicted beam stiffness (E_{app}) from MLB.

DETERMINATION OF FIBER VOLUME FRACTION

Based on the processing description provided by the pultrusion industry, micro and macro mechanical models were used to predict the laminate properties (coupons from web and flanges) and member properties (I-section). The E-glass tensile modulus and strength are 10.5×10^6 psi and 300,000 psi. The properties of the vinylester resin were experimentally determined by manufacturing resin rods and performing tensile and torsion tests (Tomblin, 1994). The matrix tensile and shear modulus were: $E_m = 0.73 \times 10^6$ psi and $G_m = 0.29 \times 10^6$ psi.

Knowing the properties of fibers and resins, a reliable measure of the fiber volume fraction was necessary to successfully determine the expected mechanical properties. There are numerous nonoptical fiber volume methods like matrix removal by combustion and solvent or acid digestion available in the literature. Various optical methods have also been developed in order to overcome the limi-

Table 5. Comparison of beam stiffness in bending.

Support Span (ft)	Experimental E_{test} (psi) (Test)	Predicted E_{app} (psi) (Apparent)	Ratio (Test)/(Apparent)
4	0.900	1.438	0.625
6	1.630	1.926	0.846
10	2.580	2.331	1.106
12	2.600	2.419	1.074
14	2.680	2.475	1.082
16	2.790	2.512	1.110
18	2.860	2.539	1.126

tation of digestion that give only the overall bulk fiber volume (Waterbury and Drzal, 1989; Jock 1986). But due to the complexity involved in these methods it seemed beneficial to predict the volume fraction theoretically. To simplify our analysis, it was assumed that the pultruded materials take the form of laminates, in which glass fibers are used as reinforcement in resin matrix. Simple formulae were developed to determine the fiber volume fraction for each layer. The layup comprises of nexus veils, fiber glass rovings and continuous strand mat.

Roving layers: The fiber volume fraction, V_f , is computed as the quotient of the area of fibers in the cross section to the total area of the cross section. The area of fibers in the cross section depends on the number of roving n , and their yield y [number of yards (0.9144 m) of roving weighing one pound (0.454 Kg)], and their density.

Volume fraction of the fibers,

$$V_f = A_f/A_c$$

Volume fraction of the matrix,

$$V_m = (1 - V_f)$$

Volume fraction of fibers in roving layers,

$$V_f = \frac{n}{t_c 2.016y\rho} \quad (13)$$

where

A_f = area of the fiber

A_c = area of the composite

V_f = volume fraction of the fibers in the roving layer

V_m = volume fraction of the matrix

n = number of fibers

y = yield in yards/pound

ρ = density in Kg/m³

Continuous strand mat and nexus veils: The continuous strand mat and nexus veil layers are modelled as random composites. The volume fraction of the nexus veils is assumed to be the same as the continuous strand mat as they do not contribute much to the properties of the laminate (they are mainly used to depress the reinforcement from the surface adding a resin rich surface to the part).

Volume fraction for continuous strand mat layers,

$$V_f^{oc} = W/\rho t_c \quad (14)$$

where

t_f = thickness of the fibers

Material

t_c = thi

ρ = de

W = we

A mic

dict the s

constitue

propertie

inate ana

(Hashin,

In this st

propertie

mechanic

material

Fourier

piecewis

Roving

transvers

dicted w

modulus

Mechani

dicted va

that for t

mechanic

with per

is obtain

where

V_f = v

G_m = m

G_f = fi

Simila

found in

Conti

tinuous s

composi

rbury and
methods it
nplify our
laminates,
e formulae
The layup
at.
quotient of
ction. The
and their
454 Kg)],

t_c = thickness of the layer
 ρ = density of the fibers
 W = weight per unit area of the continuous strand mat

MICROMECHANICS FOR STIFFNESS

A micromechanical model can be described as a mathematical tool used to predict the stiffness properties for individual laminae based on the properties of the constituents (fibers and matrix). For a laminated composite, individual laminae properties can be obtained using micromechanics which can be used for the laminate analysis. Over the years, various micromechanical models have been used (Hashin, 1962; Hoening, 1972; Mura, 1987; Christensen, 1990; Aboudi, 1991). In this study, two different approaches were used for the determination of elastic properties: (1) *mechanics of materials approach to stiffness*, based on classical mechanics of materials assumptions for the combined behavior of the constituent materials; (2) *stiffness of composites with periodic microstructure*, based on Fourier series technique and assuming the homogenization eigenstrain to be piecewise constant (Luciano and Barbero, 1994).

Roving layers: The material under investigation was assumed to be transversely isotropic and the four independent constants that needed to be predicted were: longitudinal modulus (E_1), transverse modulus (E_2) In-plane shear modulus (G_{12}), and major Poisson's ratio (ν_{12}) for the individual laminae. Mechanics of materials approach was used due to its simplicity, but the predicted values for the longitudinal and transverse modulus are upper bound and that for the shear modulus is a lower bound. To overcome the limitations of the mechanics of materials approach to stiffness, the micromechanics of composites with periodic microstructure is used. As an example, the in-plane shear modulus is obtained using,

(13)

$$G_{12} = G_m - V_f \left(\frac{S_3}{G_m} + \frac{1}{G_m - G_f} \right) \quad (15)$$

$$S_3 = 0.49247 - 0.47603 V_f - 0.02748 V_f^2$$

where

V_f = volume fraction of the fibers
 G_m = matrix shear modulus
 G_f = fiber shear modulus

(14)

Similarly, the relations to obtain each of the other mechanical properties can be found in Luciano and Barbero (1994).

Continuous strand mat and nexus layers: The elastic properties of the continuous strand mat and nexus veils are obtained assuming that they are random composites. Naughton et al. (1985) determined the elastic properties of chopped

strand mat (CSM) and woven roving (WR) experimentally using tensile and rail shear test methods. It was found that the CSM laminae did not comply with the assumption of transverse isotropy; the Young's Moduli measured in two mutually perpendicular directions were found to differ by 18 percent. Assuming properties of the CSM to be isotropic in the plane, Nielsen postulated that CSM Young's modulus could be calculated by integrating the orientation dependent Young's modulus over all possible orientations. But the equations were quite cumbersome, and Hull (1981) proposed a set of approximate relations to determine the Young's modulus, shear modulus and the Poisson's ratio, which were used in this study. The relations are:

$$\begin{aligned} E_{csm} &= 3/8E_1 + 5/8E_2 \\ G_{csm} &= 1/8E_1 + 1/4E_2 \\ \mu_{csm} &= (E_{csm}/2G_{csm}) - 1 \end{aligned} \quad (16)$$

MICROMECHANICS FOR STRENGTH

Roving layers: The prediction of composite strengths are rather difficult as compared to the elastic constants. For the prediction of elastic constants, the assumption of perfect interfacial bond is appropriate because the stresses involved are very small. Failure occurs at the weakest point in a material and a weak interface will lead to premature failure when a substantial load is expected at the interface. Unidirectional composites exhibit greater strength in the longitudinal direction as the load is mostly carried by the fibers. In other loading conditions, load sharing is about equal between fibers and matrix. The prediction of in-plane uniaxial strengths for roving layers as provided by Chamis (1984) is used in this study.

Unidirectional composites are very strong in the longitudinal direction as the load is carried by the fibers alone. As the load increases, a unidirectional fiber-reinforced composite may deform in the following stages: 1) Both fibers and matrix deform elastically; 2) Fibers continue to deform elastically, but the matrix deforms plastically; 3) Both fibers and matrix deform plastically; 4) Fibers fracture followed by fracture of the composite. Kelly and Davies (1965), Dow and Rosen (1965) and others have studied the tensile failure of fibrous composites concluding to the following approximate prediction for longitudinal tension,

$$X_t = V_f S_{fT} \quad (17)$$

where

- X_t = longitudinal tensile strength
- V_f = volume fraction of the fibers
- S_{fT} = tensile strength of the fibers

A unidirectional composite is weak in the transverse direction. In the transverse direction, load is carried mainly by the matrix. Hence, transverse tensile strength of a composite is matrix strength dominated. The prediction of the transverse tension is done using,

$$Y_t = \left[1 - (\sqrt{V_f} - V_f) \left(1 - \frac{E_m}{E_{f22}} \right) \right] S_{mT} \quad (18)$$

where

Y_t = transverse tensile strength

E_m, E_{f22} = matrix modulus and fiber modulus in the transverse direction assumed equal to E_f assuming isotropic fibers

S_{mT} = matrix strength in tension

The matrix strength in tension of vinylester is obtained as 11,800 psi from the manufacturer's design guide (Creative Pultrusions, 1988). The determination of intralaminar shear is done using,

$$S = \left[1 - (\sqrt{V_f} - V_r) \left(1 - \frac{G_m}{G_f} \right) \right] S_{mS} \quad (19)$$

where

S = shear strength

S_{mS} = matrix shear strength equal to $S_{mT}/2$.

The relation between matrix tensile and shear strength is obtained by assuming the maximum shear stress theory, which gives a more conservative value as compared to the maximum distortion theory. The matrix shear strength of Vinylester was taken as 5,900 psi.

Continuous strand mat and nexus layers: For the prediction of the strength of a lamina with random orientation, the equation developed by Hahn (1975) is used. Hahn arrived at a simple relation for the strength of a randomly oriented composite in terms of uniaxial strengths of the unidirectional composite. The strength of the random composite is shown to be equal to the average of off-axis strengths of unidirectional composite if the failure is gradual and if the rule of mixtures equation is applicable for the elastic modulus. The final equation is,

$$\frac{X_{av}}{Y_t} = \left(\frac{4}{\pi} \right) \alpha \left[1 + \frac{1}{2} \ln \left(\frac{X_t}{\alpha^2 Y_t} \right) \right], \quad \alpha \leq \left(\frac{X_t}{Y_t} \right)^{1/2} \quad (20)$$

$$\frac{X_{av}}{Y_t} = \left(\frac{4}{\pi} \right) \left(\frac{X_t}{Y_t} \right)^{1/2}, \quad \alpha > \left(\frac{X_t}{Y_t} \right)^{1/2}$$

where X_r and Y_r are the tensile strengths parallel and perpendicular to the fiber direction, respectively, and α is the ratio of the shear strength to Y_r .

MACROMECHANICS

Knowing the laminae properties from micromechanics, classical lamination theory was used to predict the laminate properties. The generalized Hooke's law relating stresses and strains in the contracted notation can be given as,

$$\sigma_i = C_{ie} \epsilon_j \quad i, j = 1, \dots, 6 \quad (21)$$

where

σ_i = stress components
 C_{ij} = stiffness matrix
 ϵ_j = strain components

The stiffness matrix has 36 constants, but due to the symmetry of the compliance matrix only 21 of the constants are independent and this matrix characterizes anisotropic materials since there are no planes of symmetry for the material properties. The material under investigation is assumed to be orthotropic and transversely isotropic in the 1-2 plane where 1,2,3 are the principal material directions. Hence, there are only four independent constants.

On-axis stiffness and compliance: Theoretical determination of the E_1 , E_2 , ν_{12} and G_{12} for a unidirectional composite lamina using a micromechanics approach was discussed previously. The stress-strain relations in an orthotropic material in a state of plane stress in terms of stiffnesses are given as,

$$\begin{pmatrix} \sigma_1 \\ \sigma_2 \\ \sigma_6 \end{pmatrix} = \begin{bmatrix} Q_{11} & Q_{12} & 0 \\ Q_{12} & Q_{22} & 0 \\ 0 & 0 & Q_{66} \end{bmatrix} \begin{pmatrix} \epsilon_1 \\ \epsilon_2 \\ \epsilon_6 \end{pmatrix} \quad (22)$$

where the stiffness components Q_{ij} ($i, j = 1, 2, 6$) can be written in terms of engineering constants as,

$$Q_{11} = \frac{E_1}{1 - \nu_{12}\nu_{21}}, \quad Q_{22} = \frac{E_2}{1 - \nu_{12}\nu_{21}} \quad (23)$$

$$Q_{12} = \nu_{12}Q_{22} = \nu_{21}Q_{11}, \quad Q_{66} = G_{66}$$

The strain-stress relations in terms of compliance are given by,

where
stands

The sti
curvatu
ing pro
 α_{ij} . Th
nate gi
gineeri
(inate) t
tensile
a lamin
based o
parison
Tables

The s
MLB (
stiffnes

where

$\bar{A}_i =$
 $[\alpha] =$
 $\bar{D}_f =$
 $[\delta] =$

The ma
quantit
ties of a

$$\begin{pmatrix} \epsilon_1 \\ \epsilon_2 \\ \epsilon_6 \end{pmatrix} = \begin{bmatrix} S_{11} & S_{12} & 0 \\ S_{12} & S_{22} & 0 \\ 0 & 0 & S_{66} \end{bmatrix} \begin{pmatrix} \sigma_1 \\ \sigma_2 \\ \sigma_6 \end{pmatrix} \quad (24)$$

where the compliance components S_{ij} ($i, j = 1, 2, 6$) in terms of engineering constants are,

$$\begin{aligned} S_{11} &= \frac{1}{E_1}, & S_{22} &= \frac{1}{E_2} \\ S_{12} &= -\frac{\nu_{12}}{E_1} = -\frac{\nu_{21}}{E_2}, & S_{66} &= \frac{1}{G_{12}} \end{aligned} \quad (25)$$

The stiffness matrix Q_{ij} is integrated with stress resultants, in-plane strains and curvatures to obtain the extensional stiffness matrix A_{ij} . The laminate engineering properties are obtained by inverting the A_{ij} matrix to the compliance matrix α_{ij} . The quantities in the compliance matrix divided by the thickness of the laminate give the engineering properties E_x , E_y , G_{xy} and ν_{xy} . Having obtained the engineering properties using micromechanics (laminae) and macromechanics (laminate) these quantities are compared to the experimentally obtained values for tensile and shear stiffnesses shown in Tables 1 and 2. To predict the strength of a laminate, a commercially available software GENLAM was used, which is based on Tsai-Wu failure criterion for the last ply failure (LPF) analysis. A comparison of the stiffness and strength properties from the predictions are shown in Tables 3 and 4.

BEAM BEHAVIOR

The structural response of the I-section under bending loads is predicted using MLB (Barbero et al., 1993) to compute the bending stiffness D and the shear stiffness F . The bending stiffness is given by,

$$D = 2\bar{A}_f \left(\frac{h}{2}\right)^2 + \frac{h^2}{12} \bar{A}_w + 2b\bar{D}_f \quad (26)$$

where

$$\begin{aligned} \bar{A}_i &= 1/\alpha_{11} \\ [\alpha] &= [A_i]^{-1} \quad i = \text{flange or web} \\ \bar{D}_f &= 1/\delta_{11} \\ [\delta] &= [D_f]^{-1} \end{aligned} \quad (23)$$

The matrices $[D]$, and $[A_i]$ are obtained using macromechanics (CLT). The quantities \bar{A}_i , \bar{D}_f are numbers, not matrices and the over-line indicates properties of a panel (flange or web). D is the bending stiffness of the I-section. For an

I-section, the shear stiffness of the flange is neglected and the shear correction factor is approximately equal to 1 (Barbero, 1991). Therefore, shear stiffness is,

$$F = \bar{F}_w = \frac{1}{\alpha_{66}} \quad (27)$$

Using the bending and shear stiffness from Equations (26) and (27) the deflection is predicted using,

$$\delta = \frac{PL^3}{48D} + \frac{PL}{4F} \quad (28)$$

The apparent modulus of elasticity is computed using,

$$E_{app} = \frac{PL^3}{48I\delta} \quad (29)$$

and compared to experimental results in Table 5.

CONCLUSIONS

Based on manufacturer's process description, simple formulae can be used for the determination of fiber volume fraction instead of cumbersome techniques like acid digestion, optical methods, and others. Experimental procedures for the determination of tensile and shear properties are simple, with the exception of Iosipescu shear test method due to the complexity of its specimen manufacture. For shear properties, it is recommended that torsion test be used for shear stiffness and Iosipescu test for shear strength. Micromechanics, based on periodic microstructure, is a reliable tool for the prediction of laminae properties, which on further combining with macromechanics renders sufficiently accurate predictions for the laminate properties. Analytical predictions for laminate properties show good agreement with experimental results, validating the assumptions in this study. For the beam bending tests, predictions using MLB agreed well with experimental results for span lengths over 10 feet.

ACKNOWLEDGEMENT

This project was sponsored by NSF grant 8802265 and WVDOH grant RPT699. Creative Pultrusions, Inc. supplied the materials used in this work. Their support is gratefully acknowledged.

REFERENCES

- Aboudi, J. 1991. "Mechanics of Composite Materials," Netherlands: Elsevier Science Publishers.
- Adams, D. F. and D. E. Walrath. 1987. "Further Development of the Iosipescu Shear Test Method," *Experimental Mechanics*, 27(2):113-119.
- Admad, S. H. and J. M. Plecnik. 1989. "Transfer of Composites Technology to Design and Construction of Bridges," Long Beach, CA: California State University, 90840.

- Barbero, E. J. 1991. "Pultruded Structural Shapes—From the Constituents to the Structural Behavior," *SAMPE Journal*, 27(1):25–30.
- Barbero, E. J. and H. V. S. GangaRao. 1991. "Structural Applications of Composites in Infrastructure," *SAMPE Journal*, Part 1, Vol. 27, No. 6, November/December, Part 2, Vol. 28, No. 1, January/February, 1992.
- Barbero, E. J., R. Lopez-Anido and J. F. Davalos. 1993. "On the Mechanics of Thin-Walled Laminated Composite Beams," *Journal of Composite Materials*, 27(8):806–829.
- Chamis, C. C. 1984. "Simplified Composites Micromechanics Equations for Strength, Fracture Toughness, and Environmental Effects, NASA TM-83696.
- Christensen, R. M. 1990. "A Critical Evaluation for a Class of Micromechanics Models," *Journal of Mech. Phys. Solids*, 38(3):379–404.
- Creative Pultrusions. 1988. "Design Guide," Alum Bank, PA: Creative Pultrusions Inc.
- Davalos, J. F., J. R. Loferski, S. M. Holzer and V. Yadama. 1991. "Transverse Isotropy Modeling of 3-D Glulam Tiber Beams," *Journal of Materials in Civil Engineering*, 3(2):125–139.
- Dow, N. F. and B. W. Rosen. 1965. "Evaluations of Filament-Reinforced Composites for Aerospace Structural Applications, NASA CR-207, April.
- GangaRao, H. V. S. and E. J. Barbero. 1991. "Construction: Structural Applications," *International Encyclopedia of Composites*, Vol. 6, 173–187. S. M. Lee, Ed., New York, NY: VCH Publishing.
- Hahn, H. T. 1975. "On Approximation for Strength of Random Fiber Composites," *Journal of Composite Materials*, 9(10):316–326.
- Hashin, Z. 1962. "The Elastic Moduli of Heterogeneous Materials," *Journal of Applied Mechanics*, 29, Transactions ASME, 84(E), pp. 143–150.
- Hoening, A. 1979. "Elastic Moduli of a Non-Randomly Cracked Body," *International Journal of Solids and Structures*, 15:137–154.
- Hull, D. 1981. "An Introduction to Composite Materials," Cambridge University Press, ISBN 0-521-28392-2.
- Iosipescu, N. 1967. "New Accurate Procedure for Single Shear Testing of Metals," *Journal of Materials*, 2(3):537–566.
- Iyer, S. L. 1991. "Advanced Composite Materials in Civil Engineering Structures," *Proceedings of the Specialty Conference*, Las Vegas, NV, January. New York, NY: American Society of Civil Engineers.
- Jock, C. P. 1986. "Quantitative Optical Microscopy Fiber Volume Methods for Composites," *Journal of Reinforced Plastics and Composites*, 5(2):110–119.
- Kelly, A. and G. J. Davies. 1965. "The Principles of the Fiber Reinforcement of Metals," *Met. Rev.*, 1–77.
- Luciano, R. and E. J. Barbero, 1994. "Formulas for the Stiffness of Composites with Periodic Microstructure," *International Journal of Solids and Structures*, In press.
- Mura, T. 1987. "Micromechanics of Defects in Solids," 2nd edn. rev., Dordrecht, The Netherlands: Martinus Nijhoff.
- Naughton, B. P., F. Panhuizen and A. C. Venmuelen. 1985. "The Elastic Properties of Chopped Strand Mat and Woven Roving in G. R. Laminae," *Journal of Reinforced Plastics and Composites*, 4(2):195–204.
- Spigel, B. S., R. Prabhakaran and J. W. Sawyer. 1987. "An Investigation of the Iosipescu and Asymmetrical Four-point Bend Tests," *Experimental Mechanics*, 27(1):57–63.
- Tomblin, J. 1994. "Compressive Strength Models for Pultruded Glass Fiber Reinforced Composites," Ph.D. dissertation submitted to the Department of Mechanical and Aerospace Engineering, West Virginia University, Morgantown, WV.
- Timoshenko, S. P. and J. N. Goodier. 1988. "Theory of Elasticity," 3rd Ed. New York, NY: McGraw-Hill Book Co., Inc., pp. 309–313.
- Waterbury, M. C. and L. T. Drzal. 1989. "Determination of Fiber Volume Fraction by Optical Numeric Volume Fraction Analysis," *Journal of Reinforced Plastics and Composites*, 8(6):627–636.